Available online at www.sciencedirect.com

ScienceDirect

Procedia Engineering 158 (2016) 146 – 151

Procedia Engineering

www.elsevier.com/locate/procedia

VI ITALIAN CONFERENCE OF RESEARCHERS IN GEOTECHNICAL ENGINEERING – Geotechnical Engineering in Multidisciplinary Research: from Microscale to Regional Scale, CNRIG2016

Dynamic soil-structure interaction of bridge-pier caisson foundations

Domenico Gaudio[a,]*, Sebastiano Rampello[a]

[a]*Università di Roma La Sapienza, via Eudossiana 18, Roma 00184, Italy*

Abstract

This paper presents the main results of 3D FE dynamic analyses carried out in the time domain to assess the seismic performance of rigid and massive circular caisson foundations supporting bridge piers. Various foundations systems are subjected to a real acceleration time history. Soil behaviour is described by an elastic-plastic model capable to provide a fair estimate of nonlinear soil behaviour and hysteretic damping under cyclic loading conditions. The coupled dynamic analyses are carried out in terms of effective stresses, thus evaluating the excess pore water pressures induced by earthquake loadings. Caisson construction stages are reproduced in a simplified way. The influence of pier height and caisson slenderness on maximum and permanent displacement and rotation attained during and at the end of the seismic shaking is considered. The equivalent seismic coefficient to be adopted in a pseudo-static analysis to check the safety of the foundation against geotechnical limit states is also evaluated.

© 2016 The Authors. Published by Elsevier Ltd. This is an open access article under the CC BY-NC-ND license (http://creativecommons.org/licenses/by-nc-nd/4.0/).

Peer-review under the responsibility of the organizing and scientific committees of CNRIG2016

Keywords: bridges; caisson foundations; dynamic anayses; earthquakes; seismic coefficient

1. Introduction

In the framework of the performance-based design, the seismic performance of a structure can be evaluated by comparing specific threshold values of earthquake-induced displacements or rotations to those attained during and at the end of the seismic event. Typically, the performance of bridge-pier caisson foundation systems is evaluated via

* Corresponding author. Tel.: +39-0644585330.
E-mail address: domenico.gaudio@uniroma1.it

1877-7058 © 2016 The Authors. Published by Elsevier Ltd. This is an open access article under the CC BY-NC-ND license (http://creativecommons.org/licenses/by-nc-nd/4.0/).
Peer-review under the responsibility of the organizing and scientific committees of CNRIG2016
doi:10.1016/j.proeng.2016.08.420

direct or substructure approaches. In the direct approach, the whole system is included in a unique model and the analyses are carried out in the time domain: it is then possible to perform nonlinear 3D analyses, referring to numerical methods [1]. Conversely, in the substructure method the soil-structure interaction problem is solved separately evaluating the kinematic and inertial effects in the frequency domain: it is then possible to perform only linear analyses, and permanent displacements cannot be evaluated [2,3].

In this paper, the seismic behaviour of various caisson foundation – bridge pier systems, differing in pier height and caisson slenderness, is studied. All systems are characterised by the same static and seismic factors of safety, F_{Sv} and F_{Se}, following the procedure proposed by Zafeirakos and Gerolymos [1], in order to analyse systems with similar degrees of mobilisation of soil shear strength before and during the seismic event. Soil behaviour is described using the *Hardening Soil with Small Strain Stiffness* (*HS small*) model [4], an elastic-plastic hysteretic model available in the library of the 3D FE code Plaxis. Systems are subjected to a real acceleration time history. Results are expressed in terms of maximum and permanent pier displacements and caisson rotations, highlighting the influence of geometric and dynamic properties of the system on them. The maximum value of the horizontal seismic coefficient to be used in the pseudo-static approach to design the caisson against geotechnical ultimate limit states is also evaluated.

2. Problem definition

In Figure 1 the problem layout is shown. The behaviour of the different systems considered in the analyses is studied in the transverse direction. A linear elastic reinforced concrete circular caisson of height H and diameter D = 12 m, supporting a bridge pier of height h_s, is embedded in a 5 m thick layer of gravelly sand and a 55 m thick layer of silty clay. The water table is located at the interface between the gravelly sand and the silty clay, z_w = 5 m, and the pore water pressure regime is hydrostatic. The pier is modelled as a linear viscous-elastic single degree of freedom, with a lumped mass $m_s = m_{deck}+0.5 \cdot m_{pier}$ applied at the top; the remaining half mass of the pier is applied at the head of the caisson through a distribution of vertical pressures $\sigma_{z(0.5\ pier)}$. The pier cross section is a hollow rectangle with sides $L > B$ and thickness s.

The mechanical properties of the foundation soils are reported in Table 1, in which I_P is the plasticity index, γ is the unit weight, c' and φ' are the effective cohesion and the angle of shearing resistance, and k_0 is the coefficient of earth pressure at rest.

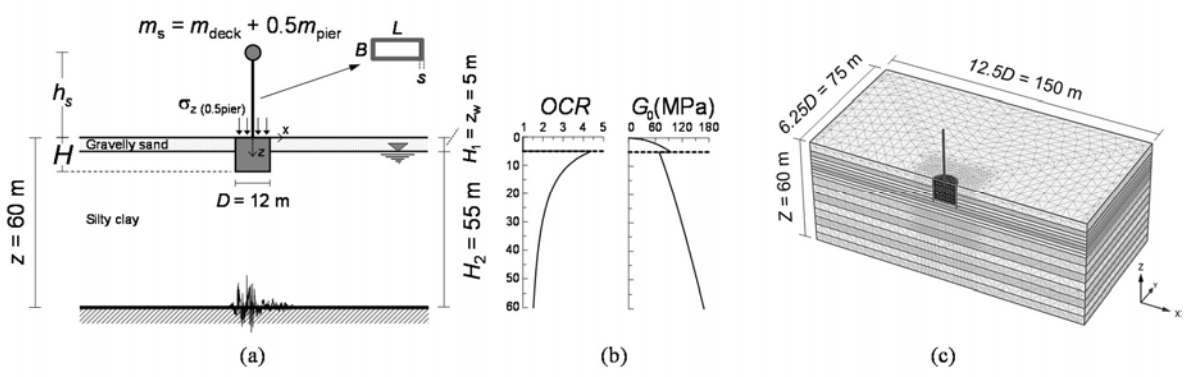

Fig. 1. Problem definition: (a) schematic layout; (b) *OCR* and G_0 profiles; (c) 3D view of the model as implemented in Plaxis 3D.

Table 1. Mechanical properties of foundation soils

Soil	I_P (%)	γ (kN/m^3)	c' (kPa)	φ' (°)	*OCR*	k_0
gravelly sand	-	20	0	30	1.0	0.5
silty clay	25	20	20	23	4.4 – 1.5	1.1 – 0.7

The profiles of overconsolidation ratio *OCR* and small-strain shear modulus G_0 are depicted in Figure 1b, the former evaluated with the Mayne and Kulhawy relationship [5], while the latter using the empirical relationship given by Hardin and Richart [6] for the gravelly sand and the one proposed by Rampello et al. [7] for the silty clay. At the soil-caisson contact, purely frictional shear resistance was assumed, with a friction angle $\delta = \tan^{-1}[2/3(\tan \varphi')]$.

The input motion, applied at the bedrock depth ($z = 60$ m), is the East-West component of Tolmezzo, Diga Ambiesta, acceleration time history, characterised by a maximum horizontal acceleration $a_{max,\,inp} = 0.316$ g, Arias intensity $I_A = 1.17$ m/s, significant duration $T_D = 5.22$ s and mean period [8] $T_m = 0.50$ s.

Caisson of varying slenderness ratio H/D and piers heights h_s were studied: specifically, all combinations of slenderness ratio $H/D = 0.5$, 1, 2 and $h_s = 15$, 30, 60 m were considered, except for the case $H/D = 2$ and $h_s = 15$ m, that can be assumed to be hardly realistic. Mechanical properties of decks and piers, such as m_{deck}, m_{pier} and pier flexural stiffness $k_{pier} = E_{cls} \cdot I/h_s^3$, in which $E_{cls} = 27.3$ GPa is the cracked reinforced concrete Young's modulus and I is the moment of inertia of interest of the pier cross section, were evaluated to obtain given values for the static and seismic factors of safety under drained conditions: $F_{Sv} = N_{ult}/N_{es} = 6$ and $F_{Se} = N_{ult,e}/N_{es} = 0.7$, where the latter provides just an estimate of the distance from the $F_{Se} = 1$ condition, [1]. Specifically, $N_{es} = (m_{deck}+m_{pier}) \cdot g$ is the vertical load acting at the head of the caisson, while N_{ult} and $N_{ult,e}$ are the bearing capacity of the caisson – soil system in static and pseudostatic conditions, evaluated using the Brinch-Hansen [9] and Froelich [10] relationships. Pseudostatic loadings acting at the head of the caisson were calculated referring to the Italian Building Code [11] elastic acceleration spectra prescribed for the site of Tolmezzo assuming a service life $V_N = 100$ years, a class of importance III, a subsoil class C ($V_{s,30} = 204$ m/s) and a topographical category T1. The period of the whole soil – caisson – pier system T_{eq}, evaluated as proposed by Tsigginos et al. [3], was used to get the spectral acceleration *Sa*. The mechanical and dynamic properties of the different systems thus obtained are given in Table 2.

Table 2. Mechanical and dynamic properties of different systems considered in this study

H/D	0.5				1				2			
h_s (m)	m_{deck} (Mg)	m_{pier} (Mg)	k_{pier} (MN/m)	T_{eq} (s)	m_{deck} (Mg)	m_{pier} (Mg)	k_{pier} (MN/m)	T_{eq} (s)	m_{deck} (Mg)	m_{pier} (Mg)	k_{pier} (MN/m)	T_{eq} (s)
15	3445.1	113.2	106.4	1.8	4160.5	134.6	169.3	1.4	-	-	-	-
30	3173.5	384.8	37.7	2.8	3806.0	489.2	78.7	2.1	4986.9	904.2	411.2	1.3
60	2159.0	1399.3	19.8	3.6	2841.1	1454.0	29.9	3.1	2374.3	3156.8	192.3	1.6

3. FE model calibration

Prior to performing the dynamic coupled analyses, a ground response analysis in free-field conditions was carried out with the code MARTA [12] assuming a nonlinear viscous-elastic soil behaviour; the curves assumed for the shear modulus decay and the damping ratio increase with the shear strain were those proposed by Seed and Idriss [13] for the gravelly sand and by Vucetic and Dobry [14] for the silty clay.

The 3D model in the code Plaxis was then calibrated for dynamic conditions against the results obtained in the aforementioned ground response analysis. To this purpose, a square column of soil of height $h = 60$ m and side $l = 10$ m was considered and a ground response analysis was carried out assuming a linear viscous-elastic soil behaviour (FEM *LE*) characterised by the operative values of shear modulus G and damping ratio ξ as provided by the analysis performed with the code MARTA. *Tied-nodes* boundary conditions [15] were also imposed in the direction of application of the input motion to force nodes at the same depth to have the same horizontal displacements. The Newmark time integration scheme was employed with the medium acceleration method, to ensure the algorithm to be unconditionally stable ($\alpha = 0.25$, $\beta = 0.5$). Maximum acceleration ratio $a_{max}/a_{max,\,inp}$ and maximum shear strain γ_{max} profiles are plotted in Figure 2, showing a very good agreement with those arising from the analysis performed with MARTA, this confirming the good calibration of the model.

The same free-field ground response analysis was carried out assuming an elastic-plastic hysteretic soil behaviour: this was described by the *HS small* model (FEM *HS small*).

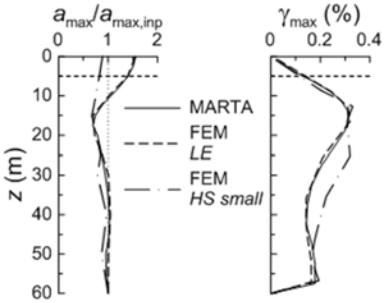

Fig. 2. Results of ground response analyses assuming different constitutive models.

In this analysis the shear modulus decay and damping ratio variation curves were calibrated against those used in the ground response analysis performed with the code MARTA, and a Rayleigh damping ratio $\xi = 1$ % was added to guarantee a minimum energy dissipation at very small strains. Accounting for elastic-plastic soil behaviour results in lower values of maximum accelerations near the ground surface, because of yielding caused by the peak shear strain attained at $z = 15$ m; similar values and profiles of γ_{max} are retrieved, this confirming the good calibration of *HS small* parameters related to changes of shear modulus and damping ratio with increasing shear strains.

4. FE coupled dynamic analyses

As reported in Figure 1a, the input motion was applied in the x direction only: this allowed to perform the 3D FE coupled analyses by modelling only half of the domain (Figure 1c). The distances of the boundaries were preliminarily calibrated by performing sensitivity analyses in pseudostatic conditions and checking that they were placed just outside the "pressure bulb" [1]. Dynamic boundary conditions are the same as previously described for free-field ground response analyses. After the initialisation of the stress state, a volumetric strain ε_v was applied to the volume that would be filled by the concrete caisson to simulate its construction stages, thus reaching active limit conditions behind the shaft lateral surface. After the activation of the caisson and the pier under drained conditions, the dynamic analysis was performed in terms of effective stresses assuming undrained conditions: at the end of earthquake loading, consolidation analyses were carried out to allow equalisation of pore water pressure. The pier is modelled with a *beam* element; at the soil-caisson contact, *interface* elements with Mohr-Coulomb failure criterion are introduced, to simulate geometric nonlinearities such as relative sliding.

Maximum and permanent dimensionless horizontal displacement of the decks $u_{x,\,deck}/h_s$ and rotation of the caissons, reported as $tan(\theta_{caisson})$, are plotted in Figure 3 versus the period ratio $T_{eq}/T_{I,soil}$, where T_{eq} is the natural period of the soil – caisson – pier system and $T_{I,soil} = 1.12$ s is the first natural period of the foundation soil column, both evaluated from the 3D analyses. Displacements and rotations decrease with increasing $T_{eq}/T_{I,soil}$, and attain their highest values for $T_{eq}/T_{I,soil} \approx 1$.

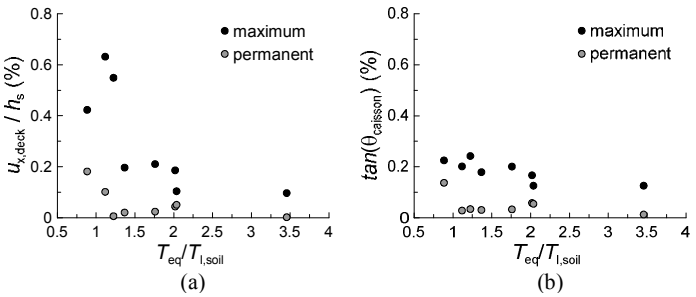

Fig. 3. Maximum and permanent (a) dimensionless horizontal deck displacement; (b) caisson rotation.

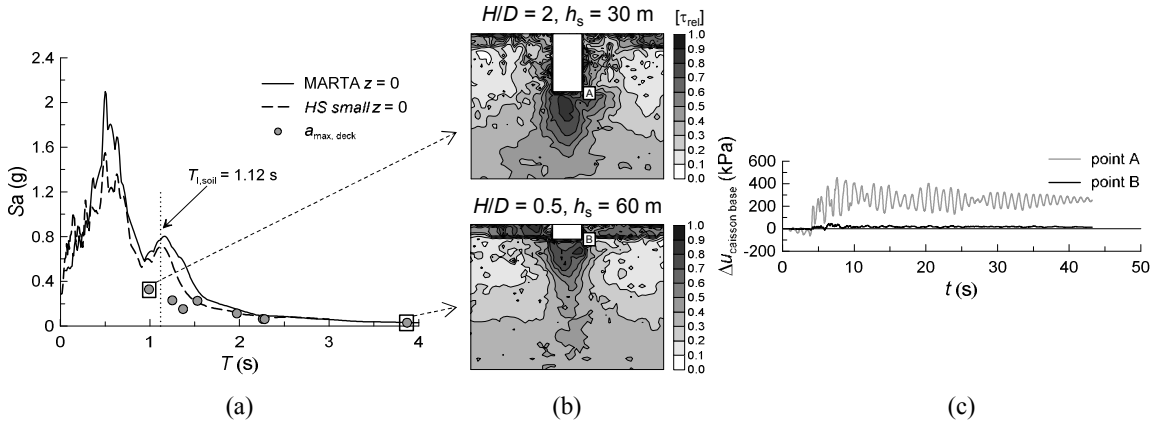

Fig. 4. Influence of $T_{eq}/T_{I,soil}$ on soil yielding at the base of the caisson: (a) maximum horizontal acceleration at the deck level compared with spectral acceleration obtained in free – field conditions; (b) contours of mobilised shear strength at the end of the seismic shaking; (c) excess pore water pressure time histories at the caisson bases.

This can be attributed to the yielding of soil foundation occurring at the caisson base, in that larger portions of soil attain full mobilisation of shear strength underneath the caisson base for values $T_{eq} \approx T_{I,soil}$ (Fig. 4). Specifically, in Figure 4a the maximum horizontal acceleration attained at the deck levels, $a_{max,\,deck}$, are plotted with full circles, together with the spectral acceleration obtained for damping ratio ξ = 5 % at the ground level in free-field conditions, under the hypotheses of nonlinear viscous-elastic (MARTA) and elastic-plastic (*HS small*) soil behaviour. The maximum accelerations at the deck levels are much lower than those deriving from the spectra for $T/T_{I,soil} \approx 1$, while follow the spectra for $T/T_{I,soil} \geq 1.5$. This is related to the higher degrees of mobilisation of the shear strength τ attained when $T_{eq}/T_{I,soil} \approx 1$, as reported in Figure 4b, where the contours of τ_{rel} at the end of the seismic shaking are plotted. Furthermore, when $T_{eq}/T_{I,soil} \approx 1$ much higher values of excess pore water pressures Δu at the base of the caisson are also attained (points A and B in Fig. 4c) .

4.1. Equivalent horizontal seismic coefficient

The dynamic analyses provide the acceleration time histories within the caisson foundation. Because of its high stiffness, the instant accelerations in the caisson can be assumed to change only with depth. This allows a simple estimate of the equivalent or average horizontal seismic coefficient $k_{h,eq}(t)$ acting on the caisson during earthquake loading. The maximum value of $k_{h,eq}(t)$ can be used in a pseudostatic analysis to evaluate the equivalent force to be applied to the caisson for its design with appropriate safety margin against geotechnical limit states.

To evaluate $k_{h,eq}(t)$ each caisson was divided into n horizontal disks of height h_i and cross section A_i. The time history of the equivalent horizontal seismic coefficient $k_{h,eq}(t)$ was estimated as the weighted average, for every time instant, of the horizontal seismic coefficient $k_{h,\,i}(t) = a_{h,\,i}(t)/g$, where $a_{h,\,i}$ is the horizontal acceleration obtained at the centre of gravity of the i^{th} disk. For constant cross section and unit weight of the caisson, the weighted average on the disk weight W_i is equal to the average on the disk height h_i:

$$k_{h,eq}(t) = \frac{\sum_i k_{h,i}(t) \cdot W_i}{W} = \frac{\sum_i k_{h,i}(t) \cdot h_i}{H} \tag{1}$$

The maximum value of the equivalent horizontal seismic coefficient, $k_{h\,eq,\,max}$, can be compared with that obtained at the ground surface in free-field conditions, $k_{h\,(gs),\,max}$, assuming a nonlinear viscous-elastic behaviour (Linear Equivalent method), an elastic-plastic behaviour as described by the *HS small* model, or using the simplified approach proposed by the Italian Building Code [11]. Fig. 5 shows that the ratio $k_{h\,eq,\,max}/k_{h\,(gs)}$ is lower than 1 in all

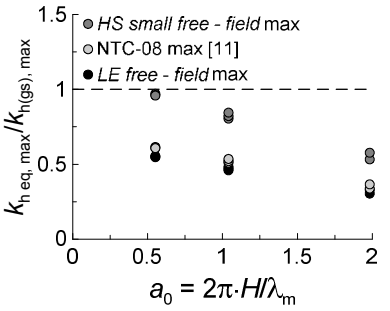

Fig. 5. Maximum seismic coefficient divided by the seismic coefficient at ground surface $k_{h\,eq,\,max}$ / $k_{h\,(gs),\,max}$ versus dimensionless wavelength a_0.

the analyses and depends on the dimensionless wavelength $a_0 = 2\pi \cdot H/\lambda_m$, where $\lambda_m = T_m \cdot V_s$ is the mean wavelength of the input motion and V_s is the shear wave soil velocity. The ratio $k_{h\,eq,\,max}/k_{h\,(gs)}$ decreases as the dimensionless wavelength a_0 increases, because of the increasing waviness of the motion applied to the caisson, this reducing the net external force applied to the caisson. Accounting for elastic-plastic soil behaviour results in higher evaluations of $k_{h\,eq,max}$.

5. Conclusions

The results presented in this paper have highlighted that the seismic performance of soil – caisson – pier systems depends on geometric and dynamic characteristics of the system. Computed values of maximum and permanent horizontal displacements of the deck, as well as caisson rotations, increase when the period ratio $T_{eq}/T_{I,soil}$ approaches unity, due to the higher degree of shear strength mobilisation underneath the caisson base. The computed ratio of the seismic coefficient acting in the caisson to the one at the ground surface, $k_{h\,eq,\,max}/\,k_{h\,(gs),}$ is always lower than unity and decreases with increasing dimensionless wavelength a_0 that expresses the ratio between the caisson height and the signal wavelength.

References

[1] A. Zafeirakos, N. Gerolymos, On the seismic response of under-designed caisson foundations, Bulletin of Earthquake Engineering 11(5) (2013) 1337–1372.
[2] N. Gerolymos, G. Gazetas, Winkler model for lateral response of rigid caisson foundations in linear soil, Soil Dynamics and Earthquake Engineering 26 (2006) 347–361.
[3] C. Tsigginos, N. Gerolymos, D. Assimaki, G. Gazetas, Seismic response of bridge pier on rigid caisson in soil stratum, Earthquake Engineering and Engineering Vibration 7 (2008) 33–44.
[4] T. Benz, Small-strain stiffness of soils and its numerical consequences, PhD Thesis, Universität Stuggart, 2006.
[5] P.W. Mayne, F.H. Kulhawy, K0 – OCR relationships in soil, Journal of the Geotechnical Engineering Division 108 (1982) 851–372.
[6] B.O. Hardin, F.E. Richart, Elastic wave velocities in granular soils, Soil Mechanics and Foundation Division 89 (1963) 33–65.
[7] S. Rampello, F. Silvestri, G. Viggiani, The dependence of G0 on stress state and history in cohesive soils, in: Pre-failure deformation of geomaterials – Measurements and application, IS-Hokkaido, Sapporo 1994, Balkema, Rotterdam (1995) 1155-1160.
[8] E.M. Rathje, N. Abrahamson, J.D. Bray, Simplified frequency content estimates of earthquake ground motions, Journal of Geotechnical Engineering 124 (1998) 150–159.
[9] J. Brinch Hansen, A revised and extended formula for bearing capacity, Bulletin No. 28 5–11, Copenaghen, 1970.
[10] X. Froelich, Beitrag fur Berechnung von Mastfundamenten, Ernest, Berlin, 1936 (in German).
[11] Ministero delle Infrastrutture, Norme Tecniche per le costruzioni, Decreto Ministero Infrastrutture 14.01.2008, Gazzetta Ufficiale della Repubblica 29, Roma, 2008 (in Italian).
[12] L. Callisto, MARTA v. 1.1: a computer program for the site response analysis of a layered soil deposit, https://sites:google.com/a/uniroma1.it/luigicallisto/attivita-1 (2015).
[13] H.B. Seed, I.M. Idriss, Soil moduli and damping factors for dynamic response analyses, Report No. EERC 70-10, Earthquake Engineering Research Center, Univ. of California, Berkeley, California, 1970.
[14] M. Vucetic, R. Dobry, Effect of soil plasticity on cyclic response, Journal of Geotechnical Engineering Division 17 (1991) 89–107.
[15] A. Amorosi, D. Boldini, A. di Lernia, Seismic ground response at Lotung: Hysteretic elasto-plastic-base 3D analyses, Soil Dynamics and Earthquake Engineering 85 (2016) 44–61.